Available online at www.sciencedirect.com
ScienceDirect
Biosensors and Bioelectronics 23 (2008) 925–931
BIOSENSORS & BIOELECTRONICS
www.elsevier.com/locate/bios

A super highly sensitive glucose biosensor based on Au nanoparticles–AgCl@polyaniline hybrid material

Wei Yan, Xiaomiao Feng, Xiaojun Chen, Wenhua Hou, Jun-Jie Zhu *

Key Laboratory of Analytical Chemistry for Life Science (MOE), School of Chemistry and Chemical Engineering, Nanjing University, Nanjing 210093, China

Received 23 May 2007; received in revised form 2 August 2007; accepted 7 September 2007
Available online 14 September 2007

Abstract

Gold nanoparticles (AuNPs) with an average diameter of 5 nm were assembled on the surface of silver chloride@polyaniline (PANI) core-shell nanocomposites (AgCl@PANI). Attenuated total reflection Fourier transform infrared spectroscopy (ATR-FTIR) suggested that AuNPs were incorporated on AgCl@PANI through coordination bonds instead of electrostatic interaction. The resulting AuNPs–AgCl@PANI hybrid material exhibited good electroactivity at a neutral pH environment. An amperometric glucose biosensor was developed by adsorption of glucose oxidase (GOx) on an AuNPs–AgCl@PANI modified glassy carbon (GC) electrode. AuNPs–AgCl@PANI could provide a biocompatible surface for high enzyme loading. Due to size effect, the AuNPs in the hybrid material could act as a good catalyst for both oxidation and reduction of H_2O_2. As the measurement of glucose was based on the electrochemical detection of H_2O_2 generated by enzyme-catalyzed-oxidation of glucose, the biosensor exhibited a super highly sensitive response to the analyte with a detection limit of 4 pM. Moreover, the biosensor showed good reproducibility and operation stability. The effects of some factors, such as temperature and pH value, were also studied.

Keywords: Glucose biosensor; AgCl@polyaniline core-shell nanocomposite; Au nanoparticles; Differential pulse voltammetry

1. Introduction

The development of materials science has brought a great momentum to bioelectroanalysis. Analysts in this field are always enthusiastic about finding new materials with good biocompatibility to improve the behavior of biosensors. Since the first report of electrical conductivity in a conjugated polymer in 1977 (Shirakawa et al., 1977), conductive polymers have attracted much interest due to their high conductivity, ease of preparation, good environmental stability, and large variety of applications in light-emitting, electronic devices, chemical sensors, separation membranes, and antistatic coatings (Liang et al., 2002; Huang et al., 1998, 2003). The most widely studied conducting polymers include polyanilie (PANI), polypyrole (PPy), and polythiophene (PTh). Among them, PANI has been proven particularly useful in the development of biosensors, because of its low cost, readily film-forming ability, chemical and electrochemical stability (Huang et al., 1986). There have been many reports on entrapping enzymes in positively charged electrosynthesized PANI films. When an enzyme carries net negative charges at a pH value which is greater than the isoelectric point, it can be adsorbed on PANI films through electrostatic interaction (Xian et al., 2006). Moreover, enzymes can be electrochemically co-deposited with aniline onto electrode surfaces (Pan et al., 2004).

Generally, an acidic condition (usually pH < 4) is required for the formation of the most highly conductive form of PANI, and this greatly restricts the applications of PANI in bioelectrochemistry, which normally needs a neutral pH environment. A kind of inorganic@conducting PANI core shell nanocomposites, silver chloride@PANI core-shell nanocomposites (AgCl@PANI), has been synthesized in our lab through a facile one-step process (Feng et al., 2006a). The obtained nanocomposites showed an excellent electrochemical behavior at a neutral pH environment. In this work, citrate-stabilized gold nanoparticles (AuNPs) with an average diameter of 5 nm were assembled on the surface of AgCl@PANI through coordination bonds to obtain the AuNPs–AgCl@PANI hybrid material. As the citrate-stabilized

* Corresponding author. Tel.: +86 25 83594976; fax: +86 25 83594976.
E-mail address: jjzhu@nju.edu.cn (J.-J. Zhu).

0956-5663/$ – see front matter © 2007 Elsevier B.V. All rights reserved.
doi:10.1016/j.bios.2007.09.002

AuNPs could provide more negative charges for anionic doping, the electroactivity of AuNPs–AgCl@PANI was better than that of AgCl@PANI. The AuNPs–AgCl@PANI was deposited on a glassy carbon (GC) electrode, and a glucose biosensor was constructed by adsorption of glucose oxidase (GOx) on the hybrid material. The enzyme could either be adsorbed on the PANI shell of AgCl@PANI or on the AuNPs in the hybrid material (Chen et al., 1998). Due to size effect, the AuNPs in the hybrid material exhibited a good catalytic effect on the reduction and oxidation of H_2O_2. The measurements of glucose can be achieved via electrochemical detection of the enzymatically liberated H_2O_2 with a detection limit of 4 pM. The super high response of the biosensor may be ascribed to the high specific surface area of AuNPs–AgCl@PANI and the size effect of AuNPs.

2. Experimental

2.1. Instruments and chemicals

Aniline, silver nitrate, Polyvinylpyrrolidone (PVP), hydrochloride (HCl), and ammonium persulfate ($(NH_4)_2S_2O_8$, APS), glucose and $HAuCl_4{\cdot}4H_2O$ were purchased from Shanghai Chemical Reagent Co. Aniline was distilled under reduced pressure. All other chemicals were of analytical grade and used without further purification. Glucose oxidase (GOx, Type VII from Aspergillus Niger, 196,000 units/g solid) was obtained from Sigma Chemical Co., and used as received. Aqueous solutions were prepared with distilled water.

Electrochemical experiments were performed on a CHI660b electrochemical workstation (Chenhua, Shanghai, China) in a three-electrode configuration. A saturated calomel electrode (SCE) and a platinum electrode served as reference and counter electrode, respectively. All potentials given below were relative to the SCE. The working electrode was a modified GC electrode.

2.2. Synthesis of AuNPs–AgCl@PANI hybrid material

AgCl@PANI nanocomposites were synthesized according to the reference (Feng et al., 2006a). $AgNO_3$ (0.012 M) and aniline (0.012 M) were added to 3% PVP aqueous solution. 5 mL of 1 M HCl aqueous solution of APS as oxidant was dropped into the above mixture under stirring at room temperature. The reaction was allowed to proceed for 24 h.

The Au colloid was prepared according to the reported method (Zhou et al., 2006) with some modifications by using KBH_4 as reductant and stabilized with sodium citrate. 5 mL of 1% $HAuCl_4$ and 10 mL of 0.03 M sodium citrate were added to 250 mL of purified water and stirred. Then 5 mL of freshly prepared 0.1 M KBH_4 was added, and the solution color changed from colorless to wine red. After the stirring was stopped, the solution was left undisturbed for 2 h. The average diameter of the obtained AuNPs was about 5 nm.

30 mL of AgCl@PANI nanocomposite solution was added into 100 mL of Au colloidal solution under stirring. The reaction was allowed to proceed for 12 h, and the resultant product was centrifuged and dispersed in water. AuNPs could be incorporated on the surface of AgCl@PANI nanocomposites, leading to the formation of AuNPs–AgCl@PANI hybrid material. The obtained hybrid material is very stable, keeping its excellent catalytic effect well on the reduction and oxidation of H_2O_2 even after 7 months.

2.3. Preparation of the modified GC electrode

A GC electrode with a diameter of 3 mm was polished to a mirror surface first with 0.05 μm α-Al_2O_3 slurry, and then ultrasonicated in distilled water and acetone successively. The cleaned electrode was dried with a stream of nitrogen immediately before use. The pretreated GC electrode was cast with 8 μL of the brown suspension of AuNPs–AgCl@PANI in water. The electrode was dried in air and then incubated in a 100 μL GOx solution (5.0 mg/mL) overnight at room temperature, and the prepared biosensor was denoted as GOx/AuNPs–AgCl@PANI/GC electrode. The enzyme electrode was stored at 4 °C, soaked in 0.1 M PBS (pH 7.0), and washed thoroughly with doubly distilled water before use.

The real surface area of the AuNPs–AgCl@PANI modified GC electrode was obtained by cyclic voltammetry (CV) using 1 mmol L^{-1} $K_3Fe(CN)_6$ as a probe at different scan rates. As the electrochemical process of $K_3Fe(CN)_6$ at the AuNPs–AgCl@PANI modified GC electrode is irreversible, the following equation exists (Bard and Faulkner):

$$I_{pa} = 299(an_a)^{1/2} A D_R^{1/2} C_o^* \upsilon^{1/2} (T = 298.2\,\mathrm{K})$$

where I_{pa} refers to the anodic peak current. For $K_3Fe(CN)_6$, D_R (diffusion coefficient) = 7.2×10^{-6} cm^2 s^{-1} in aqueous solution containing 0.1 mol L^{-3} KCl at 298.2 K (Yang et al., 2004). The value of αn_a is 0.5, which is obtained from the difference between peak and half-peak potentials ($E_p - E_{p/2} = 47.7/\alpha n_a$ mV). Then from the slope of the $I_{pa} - \upsilon^{1/2}$ relation, the real surface area can be calculated. The real surface area of the AuNPs–AgCl@PANI modified GC electrode is 0.519 cm^2, which is more than seven times larger than the geometric area of the bare GC electrode.

The amount of GOx adsorbed on the AuNPs–AgCl@PANI modified GC electrode was estimated by ultraviolet–visible (UV–vis) spectra (Ozyilmaz and Tukel). After incubating a modified electrode in the GOx solution, the intensity of the GOx adsorption peak at 280 nm decreased by 15%, indicating that there were about 75 μg of GOx had been adsorbed on the AuNPs–AgCl@PANI/GC electrode.

2.4. Characterization

The morphology of AuNPs–AgCl@PANI was observed by transmission electron microscope (TEM, JEM-1230) with an accelerating voltage of 200 kV. The sample for TEM analysis was prepared by adding drops of AuNPs–AgCl@PANI suspension onto a standard holey carbon coated copper grid. The grid was then dried in air. UV–vis absorption spectra of the aqueous dispersion of AgCl@PANI, AuNPs and AuNPs–AgCl@PANI were recorded on a UV-2401PC spectrometer. All the atten-

uated total reflection Fourier transform infrared spectroscopic (ATR-FTIR) measurements were performed on a Bruker model VECTOR22 instrument. The samples for ATR-FTIR measurements were prepared by adding drops of AgCl@PANI or AuNPs–AgCl@PANI on silicon slides. The silicon slides were then dried in air. The AuNPs–AgCl@PANI film entrapped with GOx was prepared by incubating an AuNPs–AgCl@PANI coated silicon slide in a GOx solution (5 mg/mL) overnight. The slide was then washed with distilled water and dried with N_2 stream.

3. Results and discussion

3.1. TEM of AuNPs–AgCl@PANI

The structure of AuNPs–AgCl@PANI can be confirmed directly by TEM. As shown in Fig. 1, the AuNPs have been successfully modified onto the PANI surface. The thickness of the PANI shell is about 20 nm, and the gingili-like dark spots outside the particles are AuNPs. The inside dark spots with a diameter of about 30 nm correspond to AgCl cores. When the AgCl@PANI nanocomposite was introduced into the Au colloid, the AuNPs–AgCl@PANI hybrid material was formed.

3.2. UV–vis spectra

Fig. 2 shows the UV–vis spectra of the aqueous dispersion of AuNPs, AgCl@PANI and AuNPs–AgCl@PANI. The characteristic peak of citrate-stabilized colloidal AuNPs appears at 513 nm (curve a), which is caused by the surface plasmon resonance (Lyon et al., 1998). In contrast with the PANI/Au composites hollow spheres (Feng et al., 2006b), the hybrid material still shows the surface plasmon resonance of AuNPs (curve c), and after AuNPs are assembled on the surface of AgCl@PANI, the interparticle distance between AuNPs decreases, leading to the red shift of the surface plasmon resonance (curve c). The characteristic peaks of AgCl@PANI appear at 330, 430, and 828 nm (curve b), which are attributed to π–π*, polaron–π*, and π-polaron transitions, respectively (Xia and Wang, 2002). These peaks show a shift after AuNPs are assembled (Kinyanjui and Hatchett, 2004) (curve c). As the good stability of AuNPs–AgCl@PANI, the UV–vis spectra of the hybrid material did not change with time.

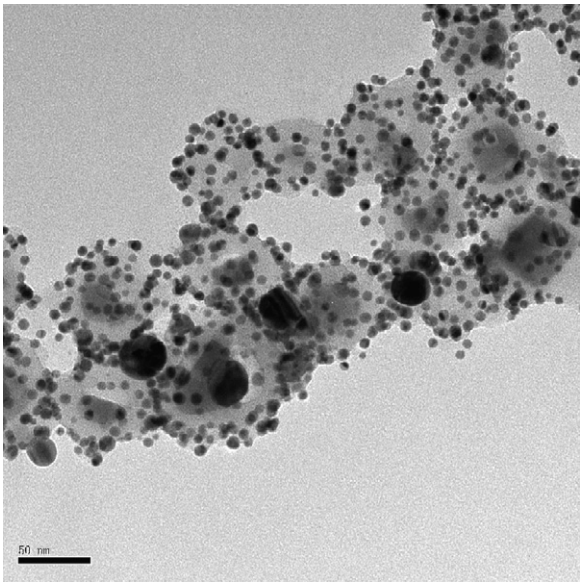

Fig. 1. TEM of AuNPs–AgCl@PANI.

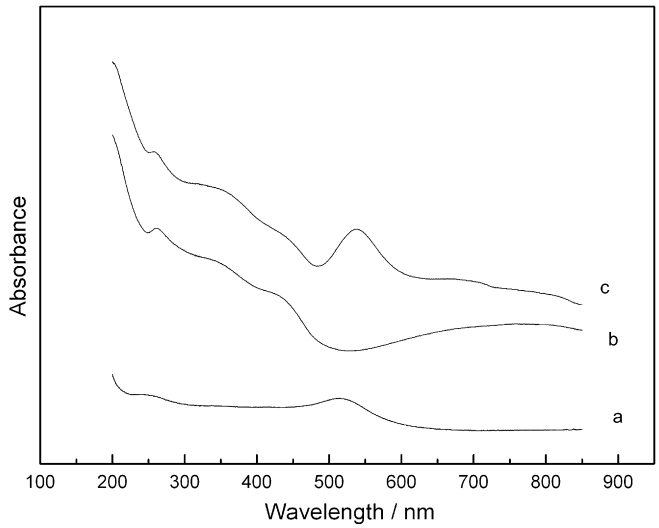

Fig. 2. UV–vis spectra of aqueous dispersion of AuNPs (a), AgCl@PANI (b) and AuNPs–AgCl@PANI (c).

3.3. ATR-FITR spectra

Fig. 3 illustrates the ATR-FTIR spectra of the AgCl@PANI film (a), and AuNPs–AgCl@PANI film without (b) and with (c) entrapment of GOx. The characteristic peak at 1571 cm^{-1} in curve (a) and (b) is related to the C=C stretching of quinoid ring (Huang and Wan, 2002). As GOx was adsorbed on the AuNPs–AgCl@PANI film, the peak at 1571 cm^{-1} shifted to the high wave-number by 12 nm in curve (c), indicating that GOx mainly located at the quinoid ring of PANI (Pan et al.,

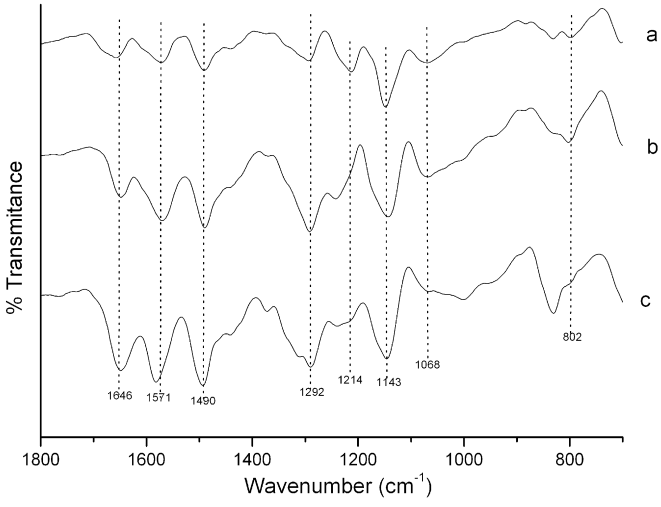

Fig. 3. ATR-FTIR spectra of the films deposited on silicon slides: AgCl@PANI film (a), AuNPs–AgCl@PANI film without (b) and with (c) entrapment of GOx.

2004). The peak at 1490 cm^{-1} corresponds to the C=C stretching of benzenoid ring (Huang and Wan, 2002), and the peak at 1292 cm^{-1} corresponds to C–N stretching mode (McCarthy et al., 2002). It can be seen in curve (a) and curve (b) that the peak corresponding to C=N stretching mode appears at 1214 cm^{-1} in AgCl@PANI film (McCarthy et al., 2002), but at 1243 cm^{-1} in AuNPs–AgCl@PANI film, implying that AuNPs are not adsorbed on AgCl@PANI nanocomposites through electrostatic interaction because the PANI shell has been doped by large amounts of negative charges. The quinoid nitrogen atoms have offered their lone pair electrons to the empty orbits of AuNPs, and coordination bonds are formed between nitrogen atoms and AuNPs. The peak at 1143 cm^{-1} is assigned to the in-plane bending of C–H (Li and Zhang, 2004), and the peak at 802 cm^{-1} is attributable to the out-of-plane bending of C–H (Trakhtenberg et al., 2005). The absorption band assignable to C=O is observed at 1646 cm^{-1}, indicating the presence of PVP (Feng et al., 2006a). The band at 1042 cm^{-1}, which is ascribed to the absorption of the $–SO_3H$ group, confirms that PANI is doped with $–SO_3H$ directly (Neoh et al., 1995). The new peak at 833 cm^{-1} in curve (c) may be caused by the GOx entrapped in the AuNPs–AgCl@PANI film.

3.4. Electroactivity of AuNPs–AgCl@PANI and its catalytic effect on oxidation and reduction of H_2O_2

Fig. 4A depicts the cyclic voltammograms obtained at a GC electrode modified with AuNPs–AgCl@PANI in buffer solutions with pH values ranging from 5.0 to 9.0. Generally, PANI is redox-active only in acid media (pH < 4) by itself. However, AuNPs–AgCl@PANI showed excellent electrochemical behavior at a neutral pH environment (curve c). Two pairs of redox peaks could be observed when pH value was 5 (curve a), and these two pairs of peaks merged and showed only one pair of broad peaks when pH value was 6 (curve b). With the increase of pH value, the peak currents decreased and ΔE_p (the peak separation between anodic and cathodic peaks) increased, suggesting the drop of the electroactivity of AuNPs–AgCl@PANI.

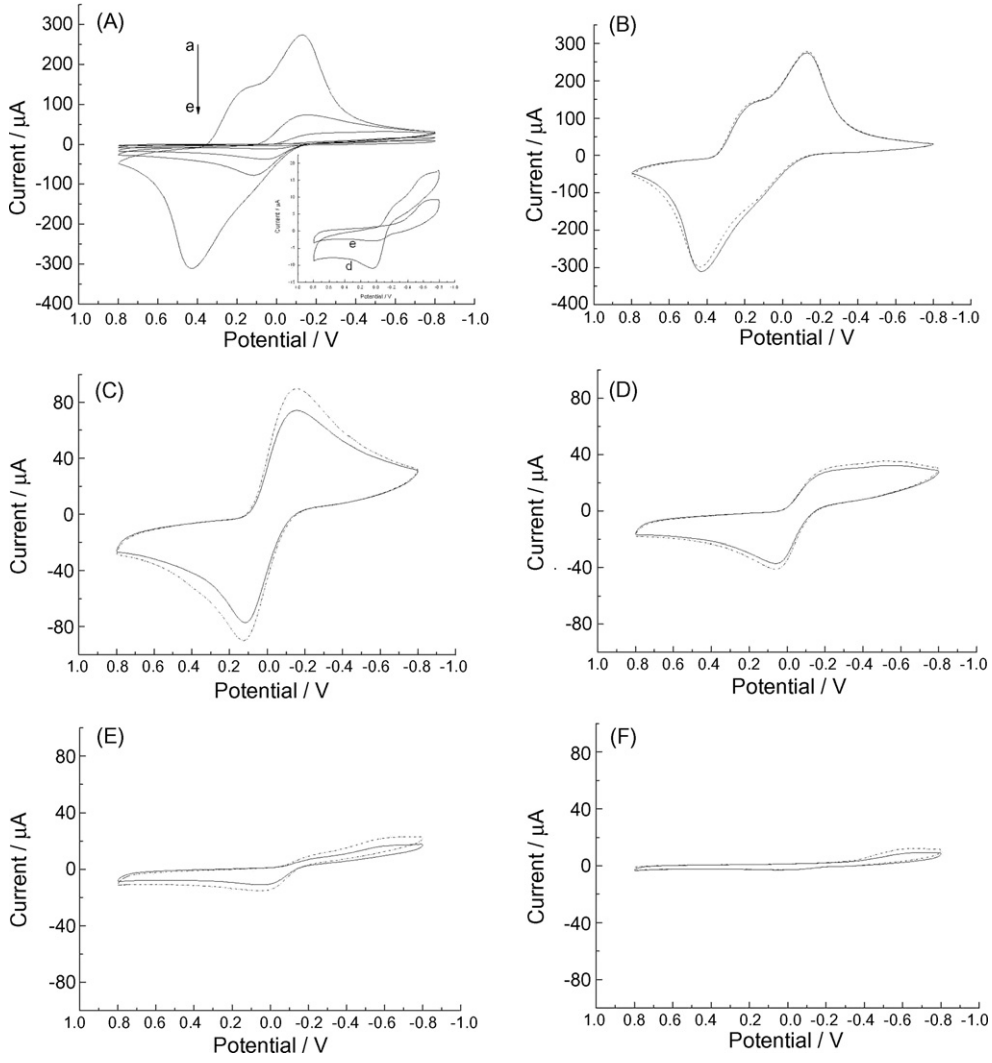

Fig. 4. Cyclic voltammograms obtained at AuNPs–AgCl@PANI modified GC electrode at pH 5 (a), 6 (b), 7 (c), 8 (d), 9 (e) (A); cyclic voltammograms obtained at AuNPs–AgCl@PANI/GC electrode without (real line) and with (dotted line) addition of 10 μM H_2O_2 in buffer solutions of different pH values: 5 (B); 6 (C); 7 (D); 8 (E) and 9 (F). (C, D, E and F are of the same scale).

It is well known that PANI exists in three well-defined oxidation states: leucoemeraldine, emeraldine and pernigraniline (Huang et al., 1986; Park et al., 2003), and the two oxidation peaks are assigned to the transition of leucoemeraldine to emeraldine salt and the transition of emeraldine salt to pernigraniline separately. Though AgCl@PANI was also reported to be electroactive at a neutral pH environment, the electroactivity of AgCl@PANI is worse than that of AuNPs–AgCl@PANI. The redox peaks of AuNPs–AgCl@PANI could still be seen when pH value was increased to 9 (curve e). It was reported that doping PANI with negatively charged sulfonate units (Bartlett and Wang, 1996), or the incorporation of negatively charged poly (acrylic acid) (Bartlett and Simon, 2000) or DNA units (Xiao et al., 2003), yields a redox-active polymer at a neutral and even basic aqueous solution. The negatively charged groups associated with the AgCl core have provided the anionic doping that made AgCl@PANI redox-active in neutral aqueous solution. The AuNPs stabilized with sodium citrate could provide more negative charges. That may be the reason why the electroactivity of AuNPs–AgCl@PANI is better than that of AgCl@PANI.

The catalytic reduction and oxidation of H_2O_2 by AuNPs–AgCl@PANI was investigated. As reported, the AgCl@PANI modified GC electrode displayed amperometric response to H_2O_2 with a detection limit of 200 μM when pH value was 7 (Feng et al., 2006a). However, it can be seen in Fig. 5 that the reduction peak currents of AuNPs–AgCl@PANI increased by 2.5 μA on addition of 1 pM H_2O_2 (curve a and b), demonstrating that AuNPs–AgCl@PANI can catalyze the reduction of H_2O_2 more efficiently than AgCl@PANI. Being different with AgCl@PANI, whose oxidative peak current decreased when H_2O_2 was added, the oxidative peak current of AuNPs–AgCl@PANI increased at the same time on addition of H_2O_2. Xian et al. believed that the incorporation of AuNPs could facilitate the electron transfer between electrode and H_2O_2 (Xian et al., 2006). Actually, it has been widely accepted that nano-scaled gold particles have some important size-dependent properties due to the quantum size effect. The surface of metallic nanoparticles is always electron deficient, and the affinity to electrons will increase with the decrease of dimension (Henglein et al., 1991). As the diameter of the AuNPs in the hybrid material is just about 5 nm, the AuNPs can act as a strong electron acceptor to adsorb electrons from H_2O_2 molecules and make them turn to the oxidized form. After adsorbing large amounts of electrons, the AuNPs turn from electron acceptors to electron donors, indicating that AuNPs–AgCl@PANI can catalyze both the oxidation and reduction of H_2O_2 efficiently.

It can be seen in Fig. 4B–F that the catalytic ability of AuNPs–AgCl@PANI changes with pH value. Almost no response was observed on the addition of H_2O_2 when pH was 5 (Fig. 4B). The maximum response of the electrode to H_2O_2 could be observed at pH 6 (Fig. 4C). With the increase of pH value, the electroactivity of AuNPs–AgCl@PANI decreased, resulting in the decrease of catalytic response (Fig. 4D–F).

3.5. Effects of pH value and temperature on the performance of the glucose biosensor

AuNPs–AgCl@PANI electrode showed no response to glucose alone, and the quantification of glucose was based on electrochemcial detection of H_2O_2 generated by enzyme-catalyzed-oxidation of the analyte. The performance of the biosensor depends not only on the activity of enzyme, but also on the electrochemical behavior of AuNPs–AgCl@PANI. The effect of pH value was studied in a range from 5.0 to 9.0, and the maximum response of GOx/AuNPs–AgCl@PANI/GC electrode to glucose occurred at pH 6.0 too.

The effect of temperature on the performance of the biosensor was investigated between 25 and 65 °C. Fig. 6 depicts the cyclic voltammograms obtained at a GOx/AuNPs–AgCl@PANI/GC electrode in pH 6.0 phosphate buffer solution (0.1 M) without any glucose at different temperatures. It can be seen that with the increase of temperature, the electroactivity of AuNPs–AgCl@PANI and the enzyme reaction rate increased

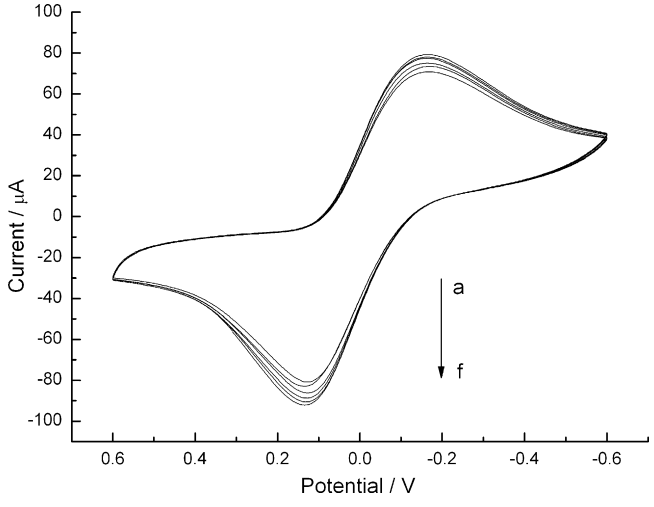

Fig. 5. Cyclic voltammograms obtained at AuNPs–AgCl@PANI modified GC electrode in 0.1 M PBS (pH 6) containing 0 pM (a), 1.0 pM (b), 5.0 pM (c), 10.0 pM (d), 15.0 pM (e), 20.0 pM (f) H_2O_2.

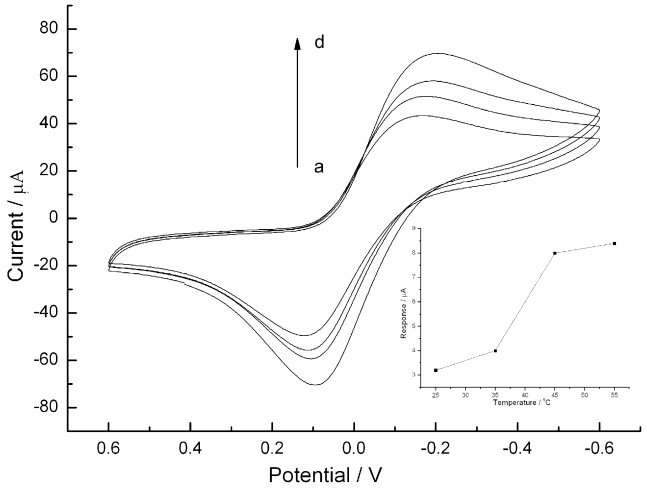

Fig. 6. Cyclic voltammograms obtained at GOx/AuNPs–AgCl@PANI/GC electrode in pH 6.0 PBS without glucose at temperature of 25 °C (a), 35 °C (b), 45 °C (c), and 55 °C (d); influence of temperature on the CV response of the biosensor to 10 μM glucose in pH 6.0 PBS (insert).

(Luo et al., 2006). The maximum response current of the GOx biosensor could be observed at about 55 °C (insert). However, when temperature was raised to 65 °C, the redox peak currents of AuNPs–AgCl@PANI kept decreasing, and it was reported that the thermal inactivation of enzyme would occur at this temperature (Luo et al., 2006).

3.6. Ameperometric determination of glucose with the biosensor

The electrochemical measurements of glucose were carried out at 55 °C in phosphate buffer solution (0.1 M) of pH 6.0. Different aliquots (0.2, 0.3, 0.4 or 0.5 μL) of 1×10^{-7} M glucose solution were successively added to 5 mL of buffer solution. To mix the glucose added, intense stirring was kept for more than 5 min. After the stirring was stopped, CV was performed until the currents did not change any more, and then differential pulse voltammetry (DPV) was immediately carried out. The biosensor exhibited super highly sensitive response to glucose with a detection limit of 4 pM. As at each time, DPV was performed when the diffusion layer had grown sufficiently, the biosensor showed good reproducibility. The relative standard deviation (R.S.D.) of five successive measurements to 10 pM glucose was 3.6%. For the interelectrode repeatability, the R.S.D. of five biosensors for detection of 10 pM glucose was 9.2%. Moreover, stored in PBS of pH 7.0 (0.1 M) at 4 °C, the biosensor still remains about 80% of its initial sensitivity after 2 weeks. GOx is considered one of the most stable enzymes, the biosensor showed a 20% response loss within 2 weeks. This could be due to an enzyme loss from the electrode surface into the PBS storing solution, which could also be estimated by UV–vis spectra. The PBS storing solution showed an adsorption peak at 280 nm, whose intensity was about 2.5% that of a GOx solution of 5.0 mg/mL. The enzyme loss from the electrode surface was estimated to be 12.5 ug.

It can be observed in Fig. 7A that with the increase of glucose concentration, a shoulder peak at 0.08 V emerges gradually. It is known that in the presence of glucose and dissolved oxygen, GOx starts to generate H_2O_2 and lactone of gluconic acid, which is hydrolyzed to gluconic acid (Ramanavicius et al., 2005). The pH value of the microenvironment of PANI will decrease in the presence of gluconic acid, explaining well the emergence of the shoulder peak, and it is because the emergence of the peak enable the GOx/AuNPs–AgCl@PANI/GC electrode does not show a wide linear range.

3.7. Interference

The glucose biosensor did not show a good anti-interference ability. However, after coated with a film of Nafion, the anti-interferent ability of the biosensor was greatly improved. The response of the biosensor was examined in the presence of different interferences with a glucose concentration of 10 pM. In the presence of ascorbic acid (10 nM), uric acid (10 nM) and cysteine (10 nM), the response of the biosensor was found to increase about 3, 2.4 and 1.8%, respectively.

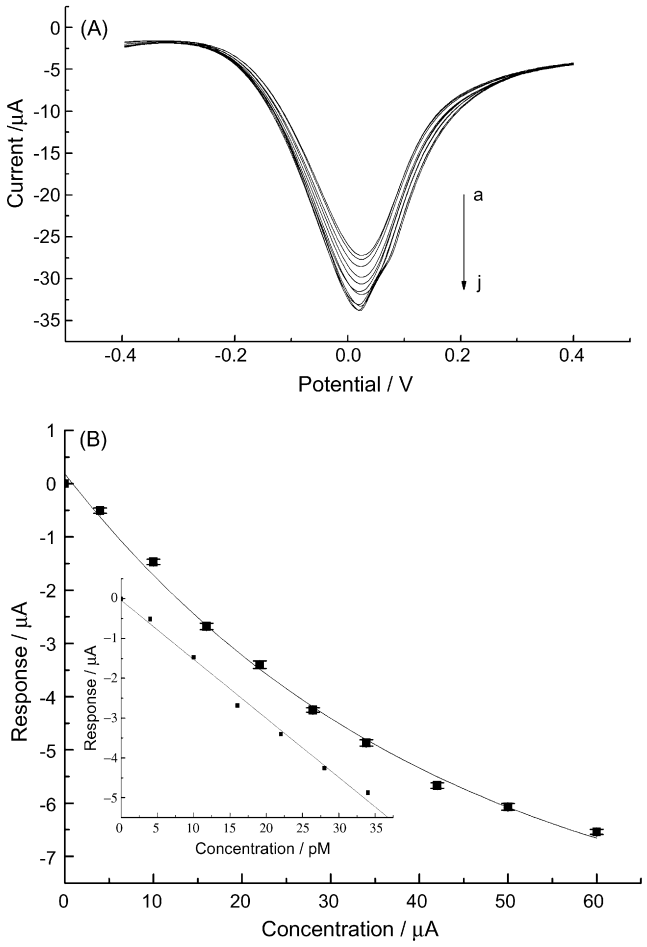

Fig. 7. Differential pulse voltammograms obtained at GOx/AuNPs–AgCl@PANI/GC electrode in 0.1 M phosphate buffer solution (pH 6.0) at 55 °C with glucose of 0 pM (a), 4 pM (b), 10 pM (c), 16 pM (d), 22 pM (e), 28 pM (f), 34 pM (g), 42 pM (h), 50 pM (i), 60 pM (j) (A); relationship between the peak current and the concentration of glucose (B).

4. Conclusion

In this paper, the AgCl@PANI core-shell nanocomposites were used for the assembly of AuNPs. After incorporation of AuNPs, the AgCl@PANI showed a greatly improved catalytic activity on the reduction and oxidation of H_2O_2 has greatly been improved. A GOx biosensor was constructed by immobilizing GOx on the AuNPs–AgCl@PANI modified GC electrode. The size effect of AuNPs and the large specific surface area of the hybrid material enabled the biosensor to exhibit highly sensitive response to glucose with a detection limit of 4 pM. Moreover, the biosensor showed high stability and good reproducibility. The AuNPs–AgCl@PANI hybrid material provides a new electrochemical platform for designing a variety of bioelectrochemical sensors of high sensitivity. However, the biosensor showed a narrow linear range in response to the analyte (4–34 pM), and a further work is needed.

Acknowledgment

We greatly appreciate the support of the National Natural Science Foundation of China for distinguished Young Scholars

(20325516), the Key Program (20635020), Creative Research Group (20521503) and General program (20575026).

References

Bard, A.J., Faulkner, L.R., 1980. Electrochemical Methods: Fundamentals and Applications. Wiley, New York.
Bartlett, P.N., Wang, J.H., 1996. J. Chem. Soc., Faraday Trans. 92, 4137–4143.
Bartlett, P.N., Simon, E., 2000. Phys. Chem. Chem. Phys. 2, 2599–2606.
Chen, X.-Y., Li, J.-R., Li, X.-C., Jiang, L., 1998. Biochem. Biophys. Res. Commun. 245, 352–355.
Feng, X., Liu, Y., Liu, C., Hou, W., Zhu, J.-J., 2006a. Nanotechnology 17, 3578–3583.
Feng, X., Mao, C., Yang, G., Hou, W., Zhu, J.-J., 2006b. Langmuir 22, 4384–4389.
Huang, J., Virji, S., Weiller, B.H., Kaner, R.B., 2003. Polyaniline Nanofibers: J. Am. Chem. Soc. 125, 314–315.
Huang, S.C., Ball, I.J., Kaner, R.B., 1998. Macromolecules 31, 5456–5464.
Huang, K., Wan, M.X., 2002. Chem. Mater. 14, 3486–3492.
Huang, W.-S., Humphrey, B.D., MacDiarmid, A.G., 1986. J. Chem. Soc., Faraday Trans. 82, 2385–2400.
Henglein, A., Mulvaney, P., Linnert, T., 1991. Chemistry of Ag. J. Chem. Soc. Faraday Discuss. 92, 31–44.
Kinyanjui, J.M., Hatchett, D.W., 2004. Chem. Mater. 16, 3390–3398.
Li, G.C., Zhang, Z.K., 2004. Macromolecules 37, 2683–2685.
Liang, L., Liu, J., Windisch, C.F., Exarhos, G.J., Lin, Y., 2002. Angew. Chem. Int. Ed. 41, 3665–3668.
Lyon, L.A., Musick, M.D., Natan, M.J., 1998. Anal. Chem. 70, 5177–5183.
Luo, X.-L., Xu, J.-J., Du, Y., Chen, H.-Y., 2006. Anal. Biochem. 334, 284–289.
McCarthy, P.A., Huang, J., Yang, S.C., Wang, H.L., 2002. Langmuir 18, 259–263.
Neoh, K.G., Pun, M.Y., Kang, E.T., Tan, K.L., 1995. Synth. Met. 73, 209–215.
Ozyilmaz, G., Tukel, S.S., 2007. Appl. Biochem. Microbiol. 43, 29–35.
Pan, X., Kan, J., Yuan, L., 2004. Sens. Acturators B 102, 325–330.
Park, M.-K., Onishi, K., Locklin, J., Caruso, F., Advincula, R.C., 2003. Langmuir 19, 8550–8554.
Ramanavicius, A., Kausaite, A., Ramanaviciene, A., 2005. Sens. Acutators B 111–112, 532–539.
Shirakawa, H., Louis, E.J., MacDiarmid, A.G., Chiang, C.K., Heeger, A.J., 1977. J. Chem. Soc., Chem. Commun. 16, 577–580.
Trakhtenberg, S., Hangun-Balkir, Y., Warner, J.C., Bruno, F.F., Kumar, J., Nagarajan, R., Samuelson, L.A., 2005. J. Am. Chem. Soc. 127, 9100.
Xia, H.S., Wang, Q., 2002. Chem. Mater. 14, 2158–2165.
Xian, Y., Hu, Y., Liu, F., Xian, Y., Wang, H., Jin, L., 2006. Biosens. Bioelectron. 21, 1996–2000.
Xiao, Y., Kharitonov, A.B., Patolsky, F., Weizmann, Y., Willner, I., 2003. Chem. Commun. 13, 1540–1541.
Yang, Z., Zhao, J., Lu, Y., Du, Z., Yang, Z., 2004. Chem. Phys. 304, 71–75.
Zhou, N., Wang, J., Chen, T., Yu, Z., Li, G., 2006. Anal. Chem. 78, 5227–5230.